Ingeniería y Competitividad
Vol 28 (3) 2026 doi: 10.25100/iyc.v28i3.15818

Vol 28 (3)

ISSN
0123-3033
e- 2027-8284

Original Article

Improvement of ttransparent and conductive thin films based on silver nanowires through mechanical and thermal treatments

Mejora de películas delgadas conductoras y transparentes de nanocables de plata mediante tratamientos mecánicos y térmicos

Angel Miguel Ardila[1] Andrés Mauricio Bernal[1]

[1]Departamento de Física, Facultad de Ciencias, Universidad Nacional de Colombia, Bogotá, Colombia.

Abstract

Introduction: ITO is widely used in transparent electrodes, but its brittleness and indium scarcity limit flexible applications. Silver nanowire thin films offer a promising alternative due to their high conductivity and mechanical flexibility.
Objective: This work evaluated thermal annealing and mechanical pressing as post-deposition treatments to enhance the electrical and optical properties of AgNW thin films.
Methods: AgNW films were deposited on glass and PET substrates by spin-coating and subsequently treated by thermal annealing (130–225 °C) or mechanical compression (2–10 tnf). Characterization included four-point probe measurements, UV–Vis spectroscopy, and SEM.
Results: As-prepared films showed sheet resistances below 30 Ω/sq and transmittances near 75 % at 530 nm. Thermal treatment at 165 °C for 22.5 min reduced sheet resistance by (50 ± 3) % without significant optical losses. Mechanical pressing at 4 tnf for 20 s achieved a (76 ± 2) % reduction, though transmittance decreased by ~9 percentage points due to nanowire densification.
Conclusions: Both treatments effectively improve the electrical performance of AgNW networks, positioning them as viable ITO replacements for flexible transparent electrodes.

Keywords: Silver nanowires, transparent electrodes, thermal annealing, mechanical pressing, ITO.

Resumen

Introducción: El ITO es ampliamente usado en electrodos transparentes, pero su fragilidad y la escasez de indio limitan aplicaciones flexibles. Las películas de nanohilos de plata (AgNW) ofrecen una alternativa prometedora por su alta conductividad y flexibilidad mecánica.
Objetivo: Se evaluaron el recocido térmico y el prensado mecánico como tratamientos post-deposición para mejorar las propiedades eléctricas y ópticas de películas de AgNW.
Métodos: Se depositaron películas de AgNW sobre sustratos de vidrio y PET por spin-coating y se trataron térmicamente (130–225 °C) o mecánicamente (2–10 tnf). Se emplearon mediciones de cuatro puntas, espectroscopía UV–Vis y SEM.
Resultados: Las películas iniciales presentaron resistencias de hoja inferiores a 30 Ω/sq y transmitancias cercanas al 75 % a 530 nm. El recocido a 165 °C durante 22,5 min redujo la resistencia en (50 ± 3) % sin pérdidas ópticas significativas. El prensado a 4 tnf durante 20 s logró una reducción de (76 ± 2) %, aunque la transmitancia disminuyó ~9 puntos porcentuales por densificación.
Conclusiones: Ambos tratamientos mejoran efectivamente el desempeño eléctrico de las redes de AgNW, posicionándolas como sustitutos viables del ITO en electrodos transparentes flexibles.

Palabras clave: Nanohilos de plata, electrodos transparentes, recocido térmico, prensado mecánico, ITO.

How to cite?

Ardila MA, Bernal AM, Improvement of ttransparent and conductive thin films based on silver nanowires through mechanical and thermal treatments. Ingeniería y Competitividad, 2026, 28(3)e-20115818

https://doi.org/10.25100/iyc.v28i3.15818

Received: 5/06/26
Reviewed: 11/07/26
Accepted: 20/08/26
Online: 14/09/26

Correspondence

ambernalf@unal.edu.co

Spanish version

Why was the study conducted?
The study was conducted to find a viable alternative to Indium Tin Oxide (ITO) for transparent electrodes widely used as anode in optoelectronic devices, which is expensive, scarce, and brittle. The researchers aimed to improve the electrical performance of silver nanowire (AgNW) thin films, fabricated via spin-coating, by applying simple post-deposition treatments.

What were the key findings?
The key findings are that both thermal annealing and mechanical pressing significantly reduce the sheet resistance of AgNW films. Thermal treatment at 165°C for 22.5 minutes achieved a ~50% reduction, while mechanical pressing with 4 tons of force for 20 seconds achieved a more substantial ~76% reduction, both without severely compromising optical transmittance.

What do these findings contribute?
These findings contribute to a practical, scalable, and effective route for enhancing AgNW transparent electrodes without the need for complex composite materials. They establish clear processing guidelines that balance electrical performance and optical transparency, reinforcing the feasibility of AgNW films as a high-performance, low-cost replacement for ITO in optoelectronic devices.

Graphical Abstract

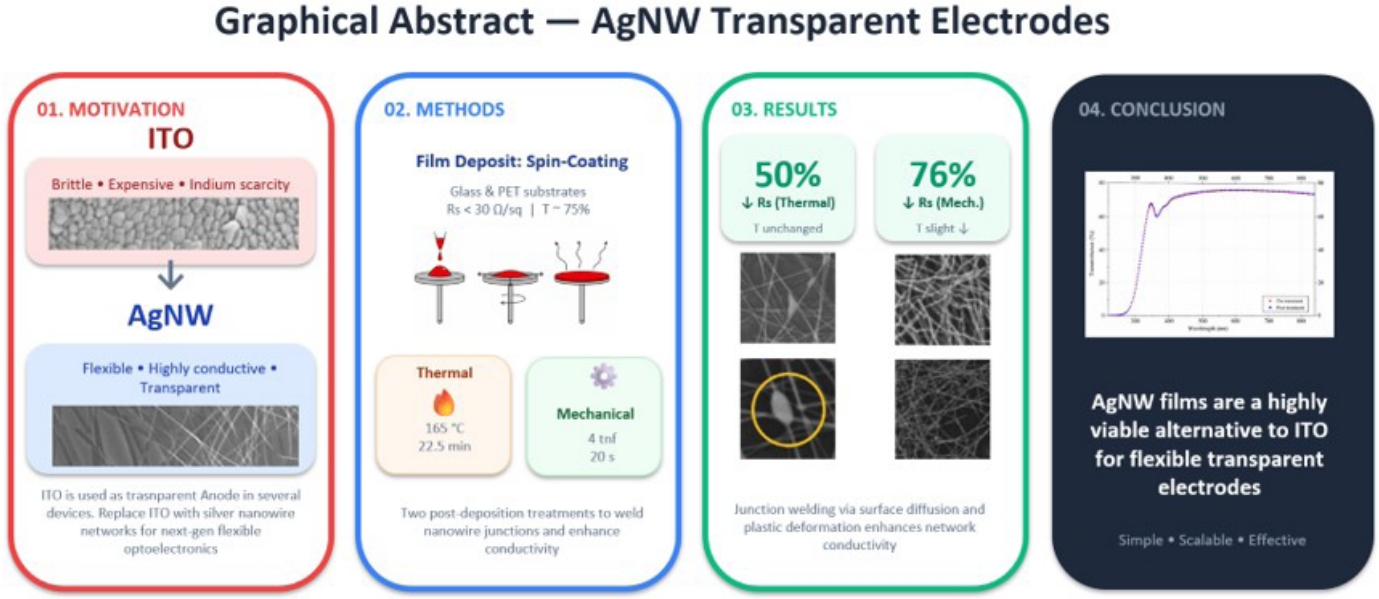

doi: 10.25100/iyc.v28i2.15818

Introduction

Optoelectronic devices such as liquid crystal displays (LCDs), solar cells, touch panels, flexible electronics, light-emitting diodes (LEDs), and organic LEDs (OLEDs) require transparent conductive films that simultaneously provide high electrical conductivity and high optical transmittance in the visible range. These properties are achieved by materials with a high density of charge carriers in the conduction band while maintaining minimal absorption of visible light. Among the most widely used materials are Transparent Conductive Oxides (TCOs), including tin oxide (SnO_2), indium oxide (In_2O_3), fluorine-doped tin oxide (FTO), and especially indium tin oxide (ITO), which exhibits high optical transmittance (T ≈ 85%) and low resistances ($R_s < 100\ \Omega/\text{sq}$) (1–4). The transparency of TCOs arises from their wide bandgap (typically > 3 eV), which prevents absorption in the visible spectrum; for ITO, this value is approximately 3.8 eV (3–5).

Despite these outstanding properties, the use of ITO presents significant limitations. Indium is a scarce and expensive element, and ITO films exhibit brittle, ceramic-like behavior, making them unsuitable for flexible devices (1,5,6). Consequently, considerable research has been directed toward alternative materials, including carbon-based nanostructures such as graphene and carbon nanotubes (7–9). However, metallic nanostructures—particularly metal nanowires—have emerged as the most promising candidates due to their excellent electrical and optical performance (2,10–12). Among these, silver nanowires (AgNWs) stand out due to the high electrical conductivity of silver (~6.3 × 10^7 S/m), the highest in all metals, along with its relatively low oxidation rate (10,13,14). AgNW-based networks have already demonstrated performance comparable to ITO in applications such as solar cells, LEDs, and flexible electronics (2,11,15). These nanostructures typically consist of diameters on the order of tens of nanometers and lengths up to hundreds of micrometers, forming percolative conductive networks that enable efficient charge transport while maintaining optical transparency (10,12,16).

Although multiple fabrication techniques have been developed for depositing AgNWs, achieving precise control over film morphology and deposition conditions remains a critical challenge (12,14,17). These parameters strongly influence key properties such as film thickness, uniformity, and connectivity. In general, increasing film thickness improves electrical conductivity due to enhanced nanowire interconnections but reduces optical transmittance due to increased light absorption and scattering. Conversely, thinner films exhibit higher transparency but poorer electrical performance (18,25). In this context, spin coating has emerged as a simple, cost-effective, and scalable technique suitable for industrial applications (11,12). This method involves depositing a small quantity of nanowire solutions onto a substrate, which is then rotated at high speeds to spread the solution via centrifugal force, forming a thin and uniform film. After deposition, thermal drying is typically applied to remove residual solvents and impurities, resulting in a random nanowire network where electrical conduction occurs at junctions and light transmission is enabled through void spaces within the network (11,14).

Recent studies have demonstrated that several post-deposition strategies can significantly improve the performance of AgNW transparent electrodes. Thermal annealing has been widely employed to remove residual organic species and promote thermally activated surface diffusion at nanowire junctions, leading to lower junction resistance and improved electrical conductivity

doi: 10.25100/iyc.v28i2.15818

(22–25). Mechanical compression has also proven to be an effective alternative by increasing the physical contact area between adjacent nanowires, reducing surface roughness, and enhancing both electrical conductivity and adhesion to the substrate (12,17,23). More recently, hybrid and composite electrode architectures incorporating AgNWs with conductive polymers, metal oxides, graphene, carbon nanotubes, or other functional materials have been developed to further improve electrical performance, mechanical stability, and environmental durability (2,12,17,23,28).

Although these approaches have demonstrated remarkable improvements in transparent conductive electrodes, they frequently involve additional fabrication steps and multiple functional materials, making it difficult to isolate the intrinsic contribution of thermal or mechanical post-deposition treatments on the AgNW conductive network itself. Furthermore, the combined effects of composite materials and post-processing often complicate the identification of the processing conditions that independently maximize the electrical performance while preserving the optical properties of the AgNW films (12,17,22–25).

In this context, the present work investigates AgNW thin films directly deposited by spin coating without incorporating additional conductive or polymeric components. This approach enables the independent evaluation of thermal annealing and mechanical compression on the electrical, optical, and morphological properties of the AgNW network. By systematically optimizing the processing temperature, exposure time, applied pressure, and pressing time, this study establishes practical processing guidelines for reducing sheet resistance while maintaining high optical transmittance, providing a simple and scalable route for the fabrication of AgNW-based transparent conductive electrodes.

Experimental

To deposit silver nanowire (AgNW), thin films, a Laurell Spin Coater and a commercial AgNW suspension (Blue Nano Inc.) were used. The nanowires had an average diameter of 35 nm and an average length of 10 µm and were dispersed in ethanol at a concentration of 1.5 wt.% with a density of 10 mg mL^{-1}, where silver represented approximately 95.5 wt.% of the solid content. AgNW thin films were fabricated by the spin-coating technique, a simple, versatile, low-cost, and scalable deposition method suitable for large-area transparent conductive electrodes.

The AgNW suspension was deposited at rotation speeds of 3000 rpm and 15000 rpm for glass and PET substrates, respectively. To improve film adhesion and reproducibility, all substrates were subjected to the same cleaning protocol consisting of ultrasonic cleaning with degreasing soap, deionized water, acetone, and isopropyl alcohol, followed by drying and oxygen plasma treatment to obtain comparable surface cleanliness and wettability. A fixed suspension volume of 60 µL was deposited by micropipette onto 4 cm^2 substrates and spin-coated for 3 min at room temperature before drying on a hot plate.

All films were fabricated using identical deposition parameters, including AgNW concentration, deposited volume, substrate preparation, spin-coating conditions, and drying procedure, to ensure reproducible film fabrication. Although spin-coated AgNW films inherently consist of randomly distributed nanowires that generate local density fluctuations, the adopted fabrication protocol produced statistically reproducible percolative networks with comparable optical and electrical

doi: 10.25100/iyc.v28i2.15818

properties. Therefore, the electrical and optical results reported throughout this work correspond to average values obtained from multiple films fabricated under identical experimental conditions.

Thermal post-deposition treatment was performed in a box-type resistance furnace, whereas mechanical treatment was carried out using a hydraulic mechanical press. Optical characterization was performed by measuring the transmittance spectra between 300 and 800 nm using a Varian Cary 5000 spectrophotometer. Morphological characterization was performed using a TESCAN VEGA3 scanning electron microscope (SEM). The electrical characterization was carried out by measuring the sheet resistance (R_s) using a Veeco FPP5000 four-point probe system. For each post-deposition condition, approximately five independently fabricated samples were measured. Sheet resistance was determined in the central region of each sample while slightly rotating the sample between successive measurements to minimize possible effects associated with preferential nanowire orientation. The reported values correspond to the average percentage variation obtained from the independent samples, and the error bars in the charts represent the corresponding standard error.

Once fabricated, AgNW films were subjected to post-deposition thermal treatment over temperatures ranging from 130 to 225 °C and exposure times between 22- and 90-min. Films deposited on PET substrates were subjected to mechanical compression by applying forces between 2 and 10 ton-force (tnf) for durations ranging from 10 to 30 s. The influence of both post-deposition treatments on film morphology, sheet resistance, and optical transmittance was subsequently evaluated.

Results and discussion

The AgNW thin films fabricated through the spin-coating method were characterized electrically, optically, and morphologically, achieving partial results comparable to those of commercial ITO films. This deposition technique allows thin films to be obtained through the centrifugal spreading of the solution, while the final physical properties can be controlled by varying the fabrication parameters. Under the conditions used in this work, AgNW thin films deposited on glass exhibited an average sheet resistance (Rs) of (24 ± 2) Ω/sq and a transmittance of (76 ± 1)%, whereas films deposited on PET showed corresponding values of (27 ± 2) Ω/sq and (63 ± 1)%, respectively. The lower transmittance observed for PET substrates is mainly attributed to the intrinsic optical properties of the polymer substrate.

Fig. 1 shows representative surface images of AgNW films deposited on glass at magnifications of 100 µm and 10 µm. The AgNW distribution observed in these micrographs is qualitatively similar to that obtained on PET substrates under the same deposition conditions. The images reveal the formation of a random percolative nanowire network that enables light transmission through the uncovered regions while electrical conduction takes place through the interconnected metallic nanowires. It is also evident that the material is not homogeneously distributed across the substrate, resulting in regions with different nanowire densities. Such local variations may increase the surface roughness, generate non-uniform current distribution, and produce junctions with different electrical contact qualities.

doi: 10.25100/iyc.v28i2.15818

This heterogeneous morphology is an intrinsic characteristic of spin-coated AgNW percolative networks and arises from the stochastic distribution of the nanowires during the deposition process. Although perfect morphological uniformity cannot be expected, the fabrication protocol was designed to maximize sample-to-sample reproducibility by maintaining identical substrate preparation, AgNW concentration, deposited solution volume, spin-coating parameters, and drying conditions. Under these controlled conditions, statistically equivalent percolative networks were consistently obtained. Consequently, the reported sheet resistance and optical transmittance values correspond to average measurements obtained from independently fabricated samples prepared under identical experimental conditions. The associated error bars represent the standard error calculated from these independent samples, thereby reflecting the inherent variability of the fabrication process rather than the uncertainty associated with repeated measurements on a single specimen.

Although morphological uniformity is desirable for transparent conductive electrodes, the objective of this work is not to eliminate the intrinsic random and percolative nature of AgNW networks. Instead, the proposed post-deposition treatments aim to improve the electrical performance by enhancing the nanowire junctions while preserving the conductive pathways responsible for charge transport. In practical optoelectronic devices, the remaining voids within the AgNW network are commonly partially infiltrated by subsequently deposited functional layers, such as PEDOT:PSS; AZO, TiO_2 or ZnO, which improve the interface with adjacent layers and facilitate device integration without requiring the conductive network itself to become a continuous metallic film (29).

Therefore, two post-deposition treatments, namely thermal annealing and mechanical pressing, were investigated to improve the morphology of the fabricated AgNW films and consequently optimize their electrical and optical performance.

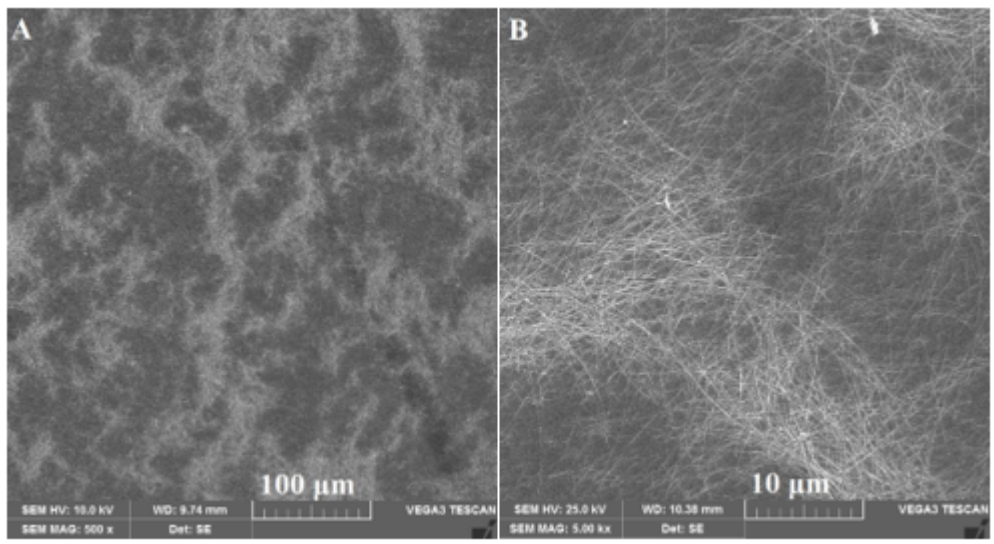

Figure. 1. Representative surface micrographs of AgNW thin films deposited on glass at (A) 100 and (B) 10μm scales. The images show the distribution of the AgNW network across the substrate and the formation of regions with different nanowire densities. The observed morphology is qualitatively similar to that obtained for AgNW films deposited on PET under the same fabrication conditions.

doi: 10.25100/iyc.v28i2.15818

A. Thermal method

Thin films were subjected to high-temperature environments, typically ranging from 100 to 250 °C, as part of a post-deposition thermal treatment. This process plays a crucial role in enhancing the electrical performance of silver nanowire (AgNW) networks. Depending on the specific temperature and exposure time, a significant increase in conductivity can be achieved. This improvement is primarily attributed to the evaporation and decomposition of residual organic compounds—such as solvents and surfactants—remaining from the synthesis and deposition processes (15,16).

Additionally, thermal treatment promotes morphological changes at the junctions between adjacent AgNWs. Unlike bulk silver, whose melting point is approximately 962 °C, AgNW networks can undergo significant junction evolution at much lower temperatures through thermally activated surface diffusion. Owing to the high surface-to-volume ratio of nanowires, atomic mobility at the surface becomes sufficiently enhanced to promote local neck formation and gradual strengthening of inter-nanowire contacts without bulk melting. As a result, the junction resistance, which dominates the overall sheet resistance of AgNW networks, is substantially reduced, leading to more efficient charge transport across the percolative network while preserving the overall nanowire morphology (22,23,26-29).

Moreover, thermal annealing can improve the adhesion between the AgNWs and the substrate, contributing to enhanced mechanical stability and durability of the films (23). However, it is important to carefully optimize the annealing conditions, as excessively high temperatures or prolonged exposure times may lead to nanowire degradation, agglomeration, or damage to temperature-sensitive substrates, especially in flexible electronic applications (26–28).

The results show that conductive increase has three different stages: i. in a temperature range from 100 to 140°C there will be a removal of organic molecules improving the contact of AgNW. As the temperature increases, thermally activated surface diffusion becomes more significant owing to the high surface energy of the nanowires (29). This process promotes atomic rearrangement at nanowire junctions, favoring neck formation and improved electrical contact between adjacent nanowires without requiring bulk melting of silver. This process leads to the fact that in many of the AgNW contacts there is a type of welding, which will facilitate the transit of charge carriers, thus decreasing the R_s. ii. As the temperature increases between 150-180°C, improvement in conductive stops, finding a minimum of R_s which would depend on the temperature and exposure time, giving the optimal values where it will obtain the greatest relative decreasing resistance. iii. For temperatures exceeding 180°C, a point will be reached at which the surface energy is minimized in such a way that it degenerates the nanostructures by breaking them and recrystallizing them in the form of a kind of Ag nanospheres. This process of maximum reduction leads to unconnected points, reducing the conductivity and raising the value of the R_s. Fig. 2 shows two different SEM images of AgNW films surfaces, Fig. 2A a surface obtained after spin-coating deposition without any post-deposit treatment and Fig. 2B a surface after thermal treatment, which resalts group of nanospheres obtained at a temperature of 225°C for 90 min, that means the destruction of AgNW is got with this temperature, a result does not desire. We tried to find out the best parameters, which are the optimal time and temperature, where it gets the maximal relative reduction of R_s.

doi: 10.25100/iyc.v28i2.15818

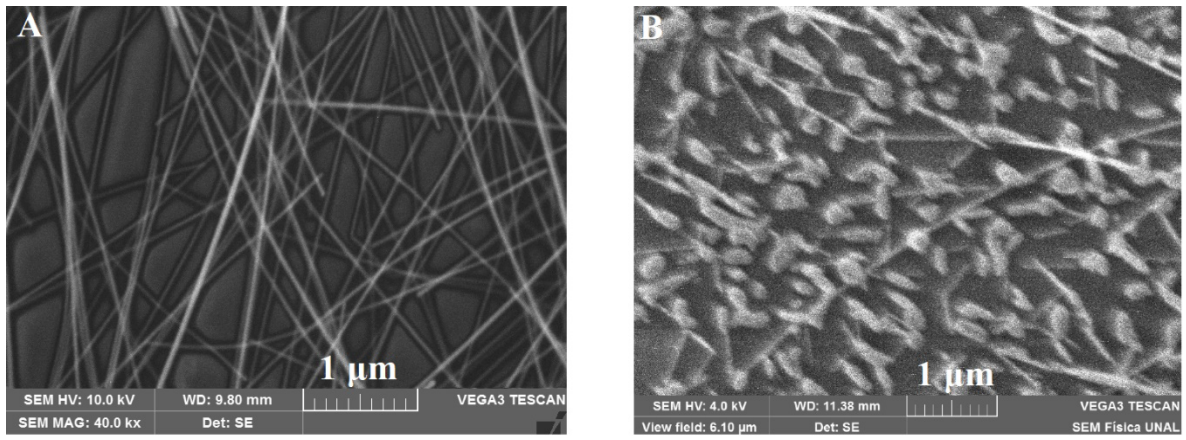

Figure 2. AgNW thin films. A) Surface obtained with spin-coating deposit technique. B) AgNW Spheroidization after thermal post-deposit treatment at 225 °C during 90 min.

To find an optimal time (t_{opt}), set a temperature of 165 °C and sweep in a time interval between 10 and 40 min. The results obtained are detailed in Fig. 3, where it shows that the relative decrease for each time was 29%, 54%, 49%, and 25%, that is, a reduction between one quarter to one-half of the initial resistance values. The curve that adjusts the relative variation of resistance as a function of time, makes clear the existence of two regions with a maximum time. The model indicates that the adjustment curve has a local maximum at 22.5min, where a theoretical decrease of up to 59% would be achieved. From there, R_s begins to decrease, going from half to a quarter of the initial resistance, the value obtained in the highest of exposure times. The optimal time chosen was t_{opt} =22.5 min, the quantity that was used to vary the annealing temperature.

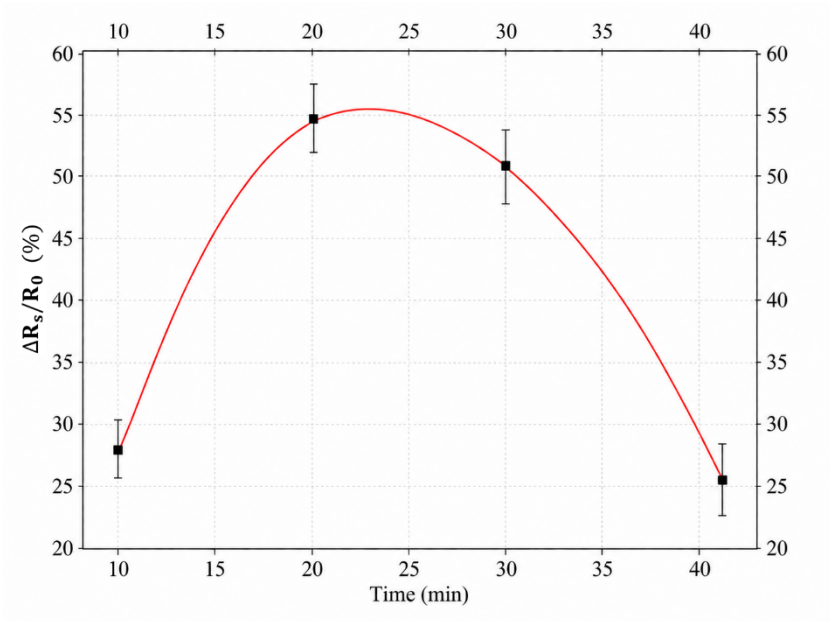

Figure 3. Relation between relative decreasing of R_s and exposure time at T=165 °C.

doi: 10.25100/iyc.v28i2.15818

The optimal time is used to make a sweep of temperatures between 130 and 190 ° C, results that are consigned in Fig. 4, where it is seen that for values between 158 and 165 °C there is a local maximum whose variation reaches 50%. Values close to this maximum, temperatures of 160 and 165 °C show an average decrease of around (51±2) %.

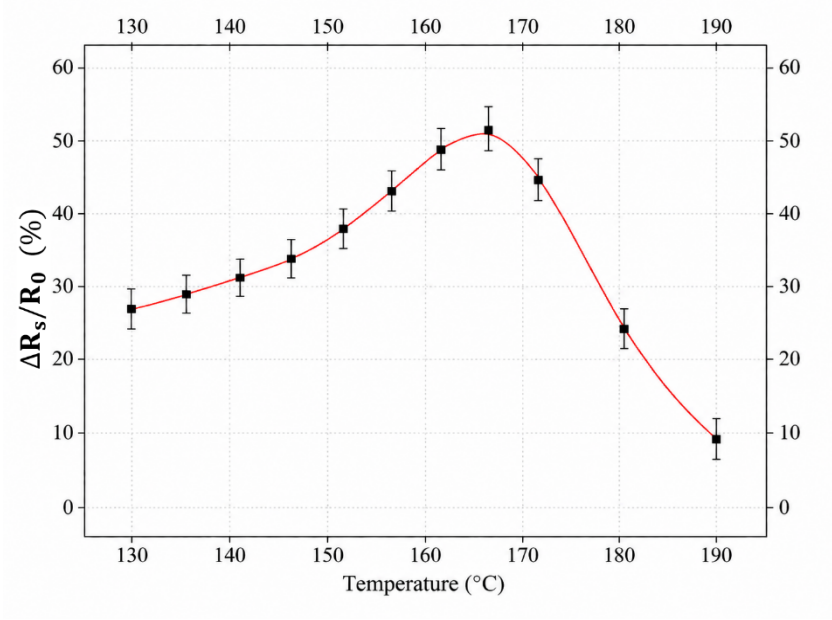

Figure 4. Relation between relative decreasing of R_s and temperature in t_{opt} 22.5min.

Fig. 4 demarcates again two different regions. The first one is located between 130 °C and the local maximum, where there is an increase in the percentage variation of the resistance as the temperature does. The second region between the maximum up to 190 °C where there is a decrease in the percentage values. Both regions shown in Figs. 3 and 4 are related to the change suffered by the nanostructured layers before the increase in temperature. In the first instance, what causes this treatment is cleaning complementary to that made in the fabrication process. The surrounding regions near the local maxima represent a balance between the removal of residual organic species and the thermally activated evolution of the AgNW junctions. Once most of the residual compounds have been eliminated, the supplied thermal energy promotes atomic surface diffusion at the nanowire junctions. This mechanism increases the effective contact area between neighboring nanowires through local neck formation, thereby substantially reducing the junction resistance, which is the dominant contribution to the overall sheet resistance of the AgNW network. Under these conditions, the nanowire network reaches its maximum electrical performance without significant morphological degradation, whereas higher temperatures promote excessive surface diffusion, leading to spheroidization and a progressive deterioration of the conductive pathways. According to the measured data, the optimal values obtained are $t_{opt} = 22.5$min and $T_{opt} = 160°C$, achieving a reduction in sheet resistance of approximately 50% (22,23,26–29).

In the way to study film morphologies after post-treatment, Fig. 5 groups some images taken with the SEM of different films subjected to this process. Fig. 5a shows the surface of a film at different scales and whose resistance reduction was 49% after being at a temperature of 165 °C for 22.5 min. It is clear how the surface has multiple points of high brightness next to the connections of

doi: 10.25100/iyc.v28i2.15818

the AgNW that did not exist in the images of films without treatment. This highlights the previously explained, there is a process of degradation of the material that causes recrystallization between connections that improves its conductivity. It is also evidenced in Fig. 5b that recrystallization can also occur around an individual wire, leading to a thickening of the diameter that does not greatly affect the transmittance.

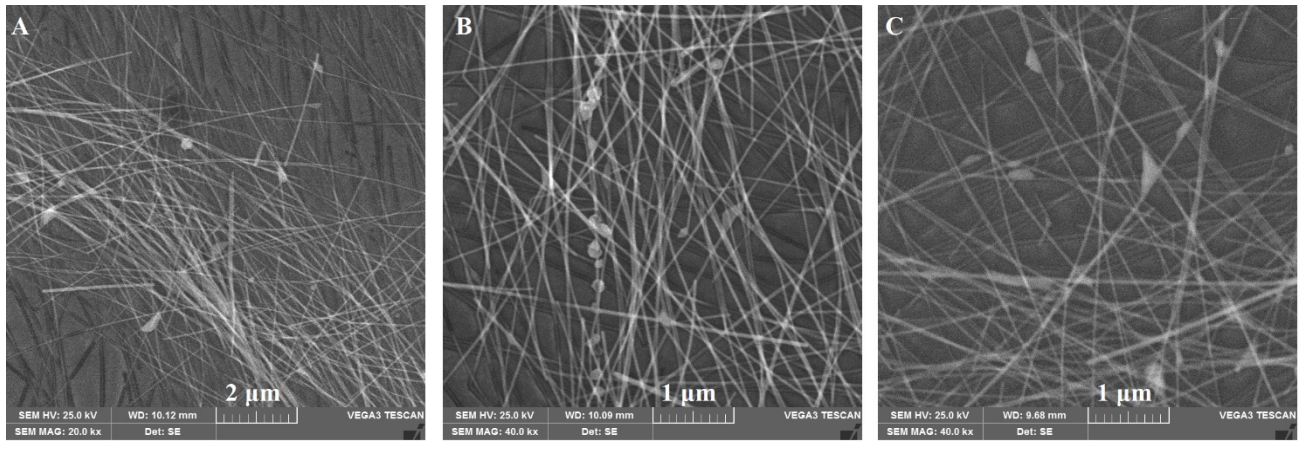

Figure 5. (a): AgNW surfaces after thermal treatment at 165 °C during 22.5 min, relatively decreasing of 49%, the bright spots observed around several nanowire intersections are consistent with localized morphological modifications produced during annealing, suggesting an increase in the contact area between adjacent nanowires. (b): It shows that the crystal can be recrystallized around an individual NW. (c): AgNW surfaces after thermal treatment at 190 °C during 22.5 min, relatively decreasing of 13%. It is evident that there is a kind of welding between connection material.

The results indicated that for very high temperatures, electrically conductive decreased significantly with respect to the maximum values found. To examine this point, Fig. 5c, which shows the surface exposed to a temperature of 190 °C during 22.5 min is analyzed. It is seen that the number of bright spots increases considerably with respect to the first images shown. In principle, what happened in this thermal regime is that the rate of nanostructured material that is degrading after atomic diffusion and redepositing around the material or between the connections is so high that it incurs a total degradation of the material, leading to processes of division or fracture of the nanostructures. This last affects the number of connections present in the nano network, which will cause the relative variation of the resistance has a decreasing trend until reaching negative percentage changes.

Finally, in Fig. 6 the material on the substrate is appreciated at a scale of 1 µm where several junctions exhibit morphological changes consistent with enhanced inter-nanowire contact after thermal annealing., where the material looks thicker because of recrystallization. This phenomenon repeats along with the surface, causing the contact resistance to be significantly reduced and resulting in a conductive improvement.

doi: 10.25100/iyc.v28i2.15818

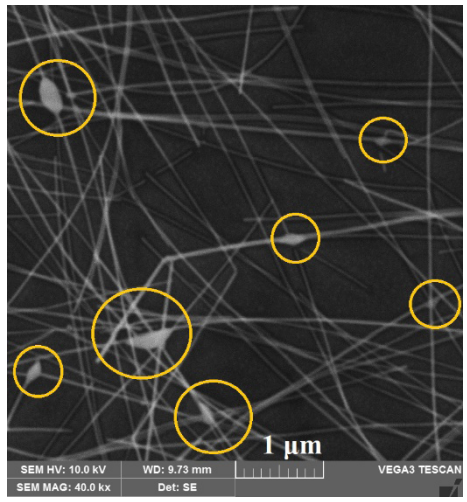

Figure 6. AgNW surface at 1 µm scale which highlights welding junction points after thermal treatment at 165 °C during 22.5 min.

In the case of optical properties, Fig. 7 shows two spectra corresponding to the average of the transmittance of thin films previous (red) and once subjected (blue) the surfaces to the thermal treatment. It shows that there are no substantial changes in the trend of the spectra, even in 550nm the values differ by a few decimals, going from 78 % to 77 %, so changes presented in this region of the spectrum are practically null. The results conclude that the variations made by the thermal method to the transmittance are insignificant in the visible.

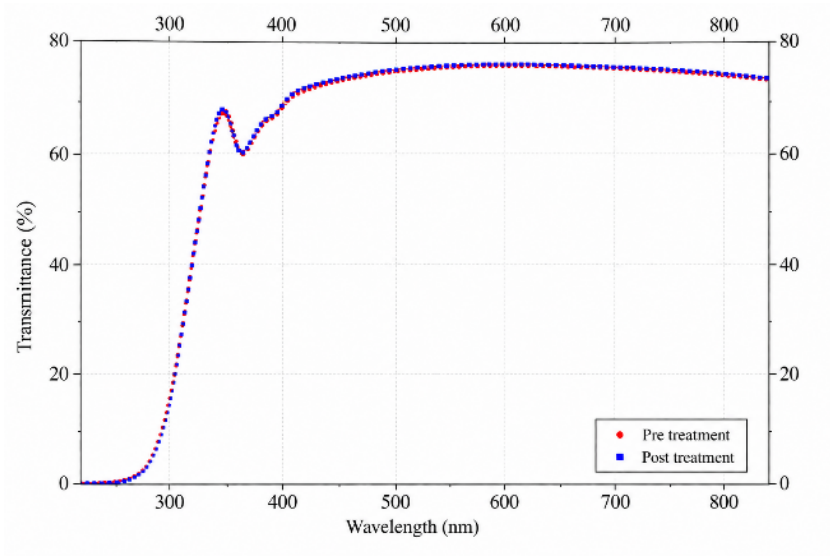

Figure 7. Comparison between average transmittance spectra before (red) and after applying thermal treatment (blue) on thin films of AgNW.

It is worth emphasizing that the improvement observed after thermal annealing does not arise from bulk melting of silver. Owing to the nanoscale dimensions of AgNWs and their high surface-to-volume ratio, atomic mobility at the nanowire surface becomes significant at temperatures far

doi: 10.25100/iyc.v28i2.15818

below the melting point of bulk silver. Consequently, local surface diffusion at nanowire junctions can reduce contact resistance without melting the entire nanowire.

B. Mechanical pressures

Some of the main limitations of AgNW thin films include poor homogeneity, arising from the random distribution of nanowires, and weak adhesion to the substrate, which can compromise both electrical performance and mechanical stability (12,17). These issues are critical in applications requiring uniform conductivity and long-term durability, such as flexible optoelectronic devices (2,20). One effective strategy to mitigate these drawbacks is the application of mechanical compression as a post-deposition treatment (23,24).

Mechanical compression not only enhances electrical conductivity but also improves film uniformity and adhesion. This process reduces surface roughness and forces the nanowire network into closer contact with the substrate, promoting stronger physical anchoring (24,28). At the nanoscale, compression significantly increases the contact area between adjacent nanowires, thereby reducing junction resistance, which is one of the dominant contributors to the overall resistivity of AgNW films (22,23). As a result, charge transport across the network becomes more efficient, leading to improved electrical performance (20,21).

Furthermore, the densification of the nanowire network induced by compression decreases the number of voids and poorly connected regions, which are typically responsible for electrical inhomogeneities (12,17). However, this process must be carefully controlled, as excessive pressure can damage the nanowire structure or reduce optical transmittance due to increased film density and light scattering (18,25-28).

The forces that were used varied from 2 to 10 tnf and applied at different times. With the pressure technique, we seek to find the physical parameters with which the highest percentage variation of the R_s is obtained, that is to find the optimal time and force. The first forces used were 2, 4, and 6 tnf and the times of 5, 10, 15, 20, and 30 s. Fig. 8 shows the percentage variation of R_s as a function of pressure time for each force applied. The red ratio was 2 tnf, the blue one for 4 tnf, and the yellow for 6 tnf. The three trends show that the decrease is practically independent of the pressure-time used, which indicates that the morphological and structural changes presented by the material become saturated after a few seconds, establishing a lower value for the R_s the rearrangement of the material on the surface. The only value that differs from the constant trends is presented in the shortest time of the force 2 tnf, time that is below the constant trend that determines the average. The average values of the percentage decrease are (40±3) %, (76±2) %, and (59±2) % for 2, 4, and 6 tnf respectively, that is, the highest percentage change is obtained for 4 tnf. Besides, it was determined that the optimal pressure time t_{opt} is 20 seconds, it was chosen so long enough, for the morphological and structural changes to occur on the surfaces without inconvenience.

doi: 10.25100/iyc.v28i2.15818

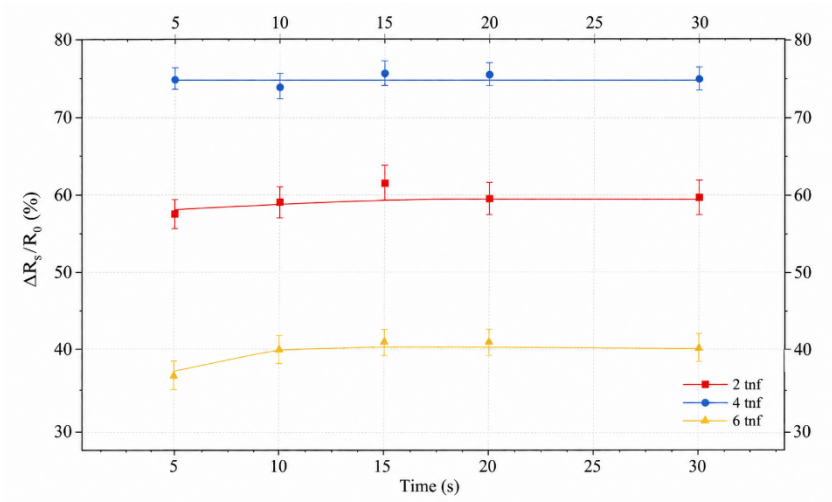

Figure 8. Relation between relative decreasing of R_s and pressure time at three fixed forces 2 tnf (red), 4 tnf (blue) and 6 tnf (yellow).

The t_{opt} is used to determine the behavior between the variations of the resistance with respect to the different forces. Fig. 9 summarizes the results obtained when we expanded this study with two new forces, 8 and 10 tnf. In all forces, there are positive values in the variation of the resistance, where it was reached that the lowest value was approximately 40% (for 2 and 10 tnf), which in themselves are good results. A maximum surround 4 tnf is achieved whit a decrease close to 75 %. Two regions can be differentiated in Fig 9. The first, concerning a region from 2 to 4 tnf, where the percentage variation with respect to the force has a positive tangent. The next one goes from the peak until the 10 tnf. This last region is presented by the pressure that begins to break the nanostructured material and by the penetration within the plastic substrate that affects the conductivity, as we will see later. If the trend continues, there will be forces high enough that will cause negative relative variations, due to the total fracture of the material or its submergence within the plastic. These results indicate that the optimal force F_{opt} is 4 tnf, which allows a balance between the increase in contact between nanowires and the rate of fractured that affects conductivity.

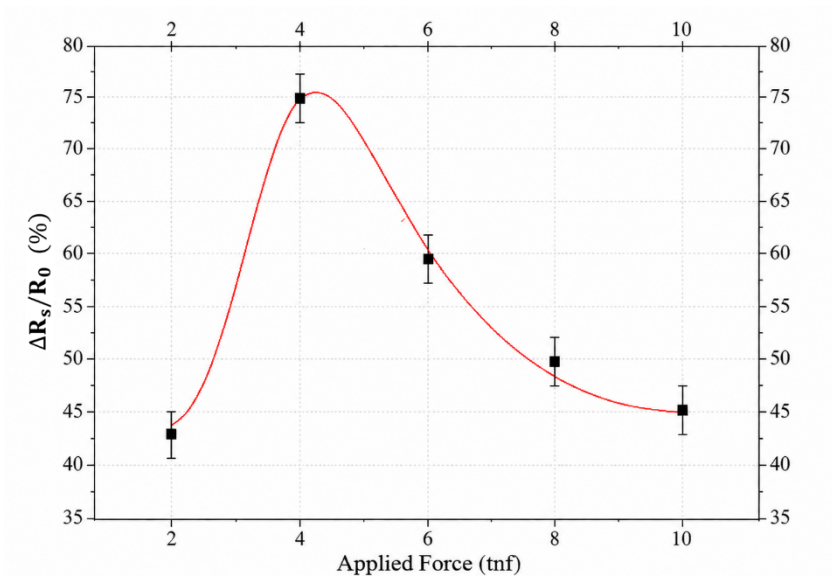

Figure 9. Relation between relative decreasing of R_s and applied force in t_{opt} 20 s.

doi: 10.25100/iyc.v28i2.15818

In Fig. 10 a series of micrographs are grouped to see the structural variation that the films have after applying the mechanical technique. It shows how the nanowires tend to curve and overlap each other after applying a force of 6 tnf. These curvatures indicate that the upper wires surround those below them, which increases the contact area and thus the conductivity of the surface. In Fig. 10a the original surface is seen, and Fig. 10b shows a film pressed, where the morphological modifications are evident by the roughness and deformations suffered by the material. Fortunately, the pressures just cause a deformation in the nanomaterial and do not break entirely the nanonetwork. Other benefits of this method are the growth of contact area between nanowires, which facilitates the electric conduction through the surface. As well, it decreases roughness across the thin film and increases adherence of AgNW on the substrate. Although with all forces probed there was a reduction in the R_s, higher forces meant a smaller reduction in the variation of the electrical parameter, as seen in Fig. 9 for 8 and 10tnf. It is not ruled out that this reduction is a product of the deterioration of nanostructures because of its fracture or breakage. In addition, Fig. 10c let us see the surface after being subjected to 10 tnf at 50 and 10 µm scales, there the substrate excels with respect to AgNW, a characteristic we did not see before treatment, which could indicate how the nanomaterial is embedded within the plastic surface, creating an isolator atmosphere that would limit the conduction. These two characteristics could be the main causes that, once past the local maximum where the greater percentage decrease obtained, this amount begins to decrease as the force increases.

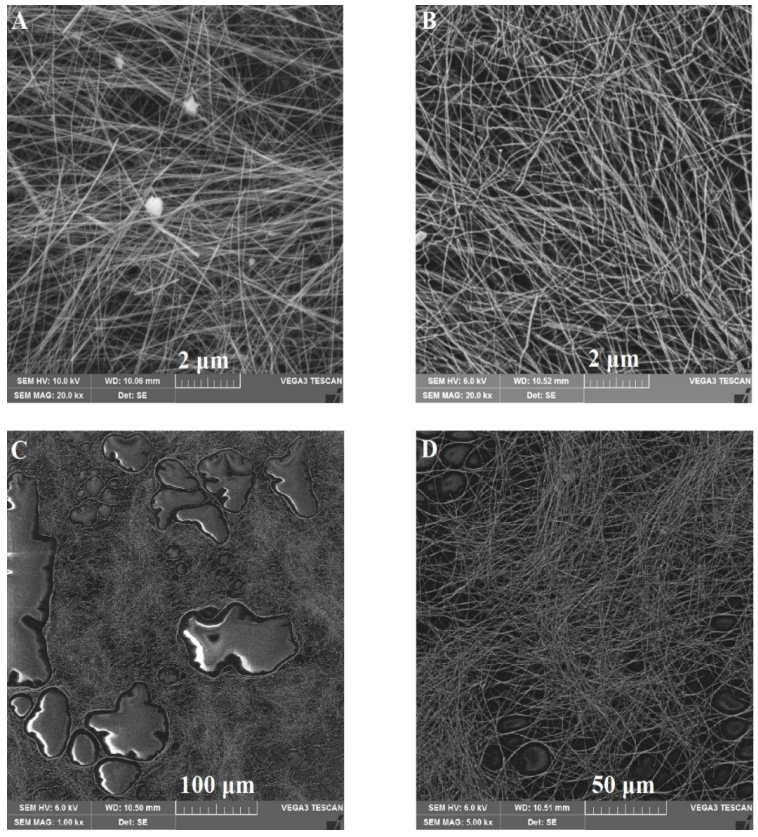

Figure 10. (Upper) Comparative between two surfaces of the same film subjected to the method with a pressure of 6 tnf (a): Before applying the method, (b) After applying mechanical pressures.

doi: 10.25100/iyc.v28i2.15818

(Lower): Surfaces of the same film after applying pressures with a force of 10 tnf, it seems that AgNW is embedded inside the plastic, with different magnifications, (c) 1 kx, (d) 5 kx.

Finally, the transmittance spectrum achieved for the different films is detailed in Fig. 11 after and before the process. Initially, the value achieved for films on the plastic substrate was 67 % at 550 nm, after applying pressures and improved the electrical properties, the average value reached for is around (59 ± 4) % in the same wavelength. The results obtained after the application of the method show that there are decreases of a few percentage points that affect the transmission of light on the surface, that could be related to the redistribution of the material that occupy most spaces on the substrate that prevents less transmission of light. In addition, although the pressure improved thin film properties, it affects permanently the physical properties of plastic substrate causing that after processing it can absorb more light.

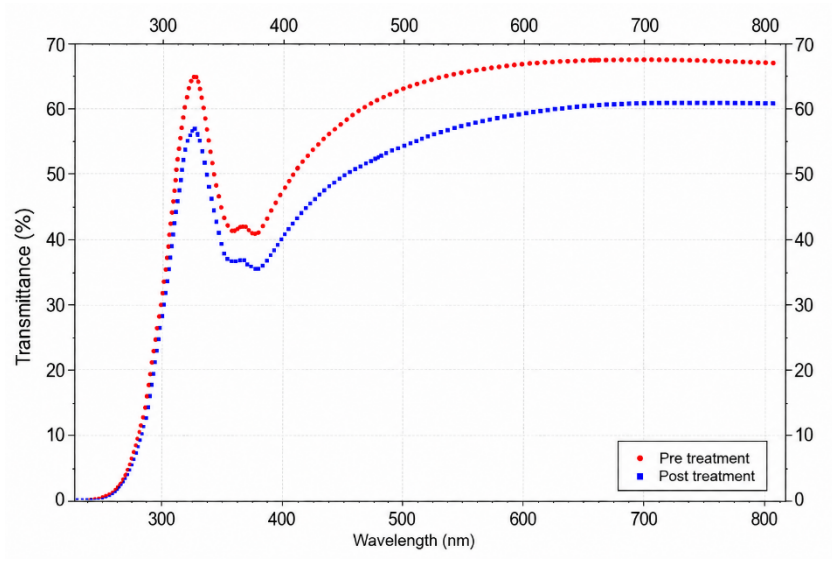

Figure 11. Average transmittance spectrum before (red) and after (blue) mechanical pressure treatment.

Conclusion

The results obtained after the manufacture of AgNW films, and the subsequent application of post-deposit treatments are very satisfactory. Thin films with R_s lower than 30 Ohm/ sq and transmittances (including the substrates) around 77 %, for glass substrate, and 67%, for plastic substrate, at 550 nm were fabricated. AgNW thin films deposited on plastic substrate are less transparent than films deposited on glass. For the thermal treatment, it was found that the maximum percentage variation of the R_s is obtained at 163 °C during 22.5 min, obtaining a reduction of (51 ± 2) %, without significantly changing its transmittance. The SEM images of the structures showed how variation was due to welding at multiple intersections of the nano-network.

For the treatment with pressures, it was found that the percentage decrease in resistance was practically independent of time, indicating that the changes in the morphology and thus in the R_s when applying pressure on the AgNW films are fast and less than the time applied in this

doi: 10.25100/iyc.v28i2.15818

work, which gives the method a plus for industrial applications. It obtained a reduction of the R_s close to (76 ± 2) % for a force of 4 tnf, affecting the transmittance by about nine percentage points at 550 nm, compared to its initial value. The SEM images show how the pressures change the nanowire structure, in the best cases, increasing the contact area with possible embedding of the nanomaterial inside the plastic substrate, improving the electrical conductivity and film adherence. The results augur silver nanostructured films as a high candidate to replace the ITO in manufacturing transparent electrodes for optoelectronic applications.

Statement of authorship contribution credits

Conceptualization – Ideas: A.M. Bernal, A.M. Ardila; Data curation: A.M. Bernal; Formal analysis: A.M. Bernal ; Funding acquisition: A.M. Ardila; Investigation: A.M. Bernal, A.M; Methodology: A.M. Bernal ; Project administration: A.M. Ardila; Supervision: A.M. Ardila; Validation: A.M. Bernal, A.M. Ardila; Visualization – A.M. Bernal; Writing – review and editing – Preparation: A.M. Bernal, A.M. Ardila.

Ethical implications: none declared; Conflicts of interest: none declared.

References

1. Patel, J., Sharma, R. K., Quijada, M. A., & Rana, M. M. (2024). A review of transparent conducting films (TCFs): Prospective ITO and AZO deposition methods and applications. Nanomaterials, 14(24), 2013.

https://doi.org/10.3390/nano14242013

2. Sharma, N., Nair, N. M., Nagasarvari, G., Ray, D., & Swaminathan, P. A review of silver nanowire-based composites for flexible electronic applications. Flexible and Printed Electronics, (2022) 7(1), 014009.

https://doi.org/10.1088/2058-8585/ac4b7d

3. Chavan, G. T., Kim, Y., Khokhar, M. Q., Hussain, S. Q., Cho, E. C., Yi, J., & Jeon, C. W. A brief review of transparent conducting oxides (TCO): The influence of different deposition techniques on the efficiency of solar cells. Nanomaterials, (2023)13,(7), 1226.

https://doi.org/10.3390/nano13071226

4. Afre, R., Sharma, N., Sharon, M., & Sharon, M. Transparent conducting oxide films for various applications: A review. Reviews on Advanced Materials Science, (2018), 53(1), 79–89.

https://doi.org/10.1515/rams-2018-0006

5. Pasquarelli, R. M., Ginley, D. S., & O'Hayre, R. Solution processing of transparent conductors: From flask to film. Chemical Society Reviews, (2011) 40(11), 5406–5441.

https://doi.org/10.1039/c1cs15031e

6. Ma, J. H., Kim, M. G., Jeong, J. H., Park, M. H., Ha, H. J., Kang, S. J., & Kang, S. J. Highly efficient ITO-free quantum-dot light emitting diodes via solution-processed PEDOT:PSS semitransparent electrode. Materials, (2023) 16(11), 4053.

https://doi.org/10.3390/ma1611405

7. Zhang, J., Chen, Z., Xu, X., Liao, W., & Yang, L. A simple and efficient approach to fabricate graphene/CNT hybrid transparent conductive films. RSC Advances, (2017) 7(83), 52555–52560.

https://doi.org/10.1039/c7ra10225h

8. Rosli, N. N., Ibrahim, M. A., Ludin, N. A., Teridi, M. A. M., & Sopian, K. A review of graphene-based transparent conducting films for use in solar photovoltaic applications. Renewable and Sustainable Energy Reviews, (2019) 99, 83–99.

https://doi.org/10.1016/j.rser.2018.09.020

9. Siwal, S. S., Saini, A. K., Rarotra, S., Zhang, Q., & Thakur, V. K. Advancements in transparent carbon nanotube films: Chemistry and imminent challenges. Journal of Nanostructure in Chemistry, (2021) 11(1), 93–130.

https://doi.org/10.1007/s40097-020-00374-5

10. Tan, D., Jiang, C., Li, Q., Bi, S., & Song, J. Silver nanowire networks: Preparation and applications. Journal of Materials Science: Materials in Electronics, (2020) 31(18), 15669–15696.

https://doi.org/10.1007/s10854-020-04171-0

11. Tokuno, T., Nogi, M., Karakawa, M., Jiu, J., Nge, T. T., Aso, Y., & Suganuma, K. . Fabrication of silver nanowire transparent electrodes at room temperature. Nano Research, (2011) 4(12), 1215–1222.

https://doi.org/10.1007/s12274-011-0162-6

12. Li, W., Zhang, H., Shi, S., Xu, J., Qin, X., He, Q., & Fahlman, M. Recent progress in silver nanowire networks for flexible organic electronics. Journal of Materials Chemistry C, (2020) 8(14), 4636–4674.

https://doi.org/10.1039/c9tc05891a

13. Dinh, D. A., Hui, K. N., Hui, K. S., Kumar, P., & Singh, J. Silver nanowires: A promising transparent conducting electrode material for optoelectronic and electronic applications. Reviews in Advanced Sciences and Engineering, (2013) 2(4), 324–345.

https://doi.org/10.1166/rase.2013.1050

14. Wang, H., Wang, Y., & Chen, X. Synthesis of uniform silver nanowires from AgCl seeds for transparent conductive films via spin-coating at variable spin-speed. Colloids and Surfaces A: Physicochemical and Engineering Aspects, (2019) 565, 154–161.

https://doi.org/10.1016/j.colsurfa.2018.12.063

15. Hu, L., Kim, H. S., Lee, J. Y., Peumans, P., & Cui, Y. Scalable coating and properties of transparent, flexible, silver nanowire electrodes. ACS Nano, (2010) 4(5), 2955–2963.

https://doi.org/10.1021/nn1005232

16. Khaligh, H. H. Silver nanowire transparent electrodes: Fabrication, characterization, and device integration (Doctoral dissertation, University of Waterloo). (2013)

17. Meena, J. S., Choi, S. B., Jung, S. B., & Kim, J. W. Advances in silver nanowire-based composite electrodes: Materials processing, fabrication, and applications. Advanced Materials Technologies, (2023) 8(19), 2300602.

https://doi.org/10.1002/admt.202300602

18. Lam, K. K., Ng, S. M., Wong, H. F., Fei, L., Liu, Y., Chan, K. H., & Mak, C. L. Effect of thickness on the optical and electrical properties of ITO/Au/ITO sandwich structures. ACS Applied Materials & Interfaces, (2020) 12(11), 13437–13446.

https://doi.org/10.1021/acsami.9b22108

19. Wang, S., Liu, H., Pan, Y., Xie, F., Zhang, Y., Zhao, J., & Gao, F. Performance enhancement of silver nanowire-based transparent electrodes by ultraviolet irradiation. Nanomaterials, (2022) 12(17), 2956.

https://doi.org/10.3390/nano12172956

20. Wang, J., Fan, J., Wan, T., Hu, L., Li, Z., & Chu, D. Recent progress in silver nanowire-based transparent conductive electrodes. Advanced Energy and Sustainability Research, (2025). 6(9), 2500033.

https://doi.org/10.1002/aesr.202500033

21. Li, J., Luo, J., & Liu, Y. Recent advances in silver nanowire-based transparent conductive films: From synthesis to applications. Coatings, (2025) 15(7), 858.

https://doi.org/10.3390/coatings15070858

22. Song, T. B., Chen, Y., Chung, C. H., Yang, Y., Bob, B., Duan, H. S., Li, G., Tu, N. G., Huang, Y., & Yang, Y. Nanoscale joule heating and electromigration enhanced ripening of silver nanowire contacts. ACS Nano, (2014) 8(3), 2804–2811.

https://doi.org/10.1021/nn406405s

23. Azani, M. R., Hassanpour, A., & Torres, T. Benefits, problems, and solutions of silver nanowire transparent conductive electrodes in indium tin oxide (ITO)-free flexible solar cells. Advanced Energy Materials, (2020) 10(48), 2002536.

https://doi.org/10.1002/aenm.202002536

24. Ding, Y., Cui, Y., Liu, X., Liu, G., & Shan, F. Welded silver nanowire networks as high-performance transparent conductive electrodes: Welding techniques and device applications. Applied Materials Today, (2020) 20, 100634.

https://doi.org/10.1016/j.apmt.2020.100634

25. Im, H. G., Jang, J., Jeon, Y., Noh, J., Jin, J., Lee, J. Y., & Bae, B. S. Flexible transparent crystalline-ITO/Ag nanowire hybrid electrode with high stability for organic optoelectronics. ACS Applied Materials & Interfaces,(2020).12(50), 56462–56469.

https://doi.org/10.1021/acsami.0c16572

26. Hu, Y., Zhang, X., Ding, H., & Hu, Y. Laser shock-enabled optical–thermal–mechanical coupled welding method for silver nanowires. International Journal of Machine Tools and Manufacture, (2024) 199, 104162.

https://doi.org/10.1016/j.ijmachtools.2024.104162.

27. Bian, M., Qian, Y., Cao, H., Huang, T., Ren, Z., Dai, X., Zhao, W., Li, J., & Yin, S. Chemically welding silver nanowires toward transferable and flexible transparent electrodes in heaters and double-sided perovskite solar cells. ACS Applied Materials & Interfaces, (2023) 15 (10), 13307–13318.

https://doi.org/10.1021/acsami.2c22864

doi: 10.25100/iyc.v28i2.15818

28. Garnett, E. C., Cai, W., Cha, J. J., Mahmood, F., Connor, S. T., Greyson Christoforo, M., Cui, Y., McGehee, M. D., & Brongersma, M. L. Self-limited plasmonic welding of silver nanowire junctions. Nature Materials, (2012), 11(3), 241–249.

https://doi.org/10.1038/nmat3238

29. Sekkat, A., Sanchez-Velasquez, C., Bardet, L., Weber, M., Jiménez, C., Bellet, D., Muñoz-Rojas, D., & Nguyen, V. H. Towards enhanced transparent conductive nanocomposites based on metallic nanowire networks coated with metal oxides: A brief review. Journal of Materials Chemistry A, (2024). 12(38), 25600–25621.

https://doi.org/10.1039/D4TA05370B

doi: 10.25100/iyc.v28i2.15818